Supplementary Figure 1. Torashima et al.

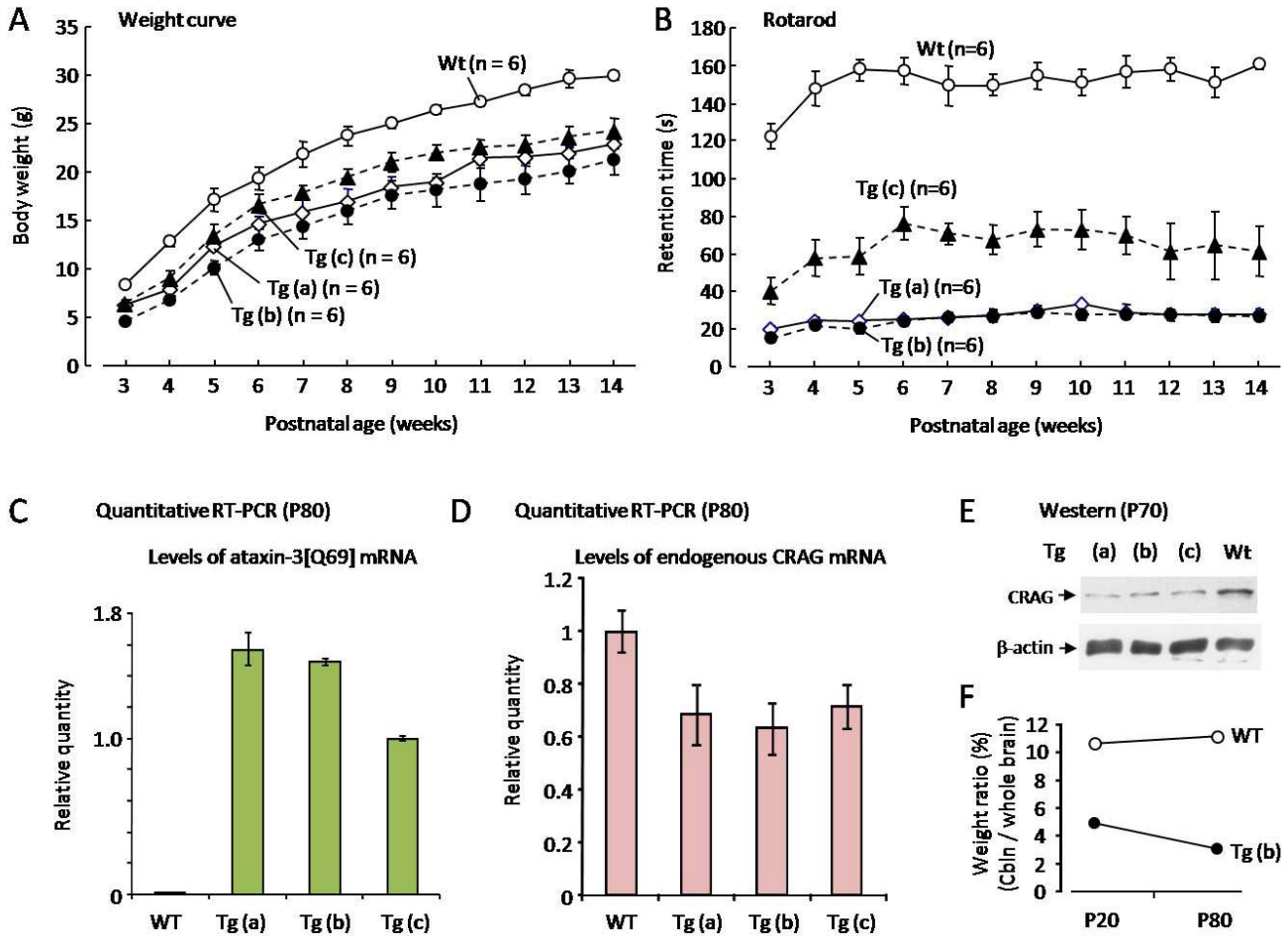

Supplementary Figure 1. Weight curve, rotarod performance and expression levels of ataxin-3 and CRAG in three different lines of polyQ model mice.

There were three founder lines of polyQ mice [(a), (b) and (c) lines]. (A, B) Weight curve (A) and rotarod performance (B) of the poly Q mice and their wild-type littermates measured at three to 14 weeks of age. Six mice in each cohort were examined. The rod was accelerated from 0 rpm and reached the maximum speed (40 rpm) in three min. (C, D) Quantitative RT-PCR analysis of ataxin-3 mRNA (C) and CRAG mRNA (D) in cerebellar extracts of three different transgenic lines. The data from eight runs of real-time PCR using 2 animals were normalized with the values of wild-type cerebellum. Although the expression levels of ataxin-3 mRNA in polyQ mouse cerebella appear to be about 100~160 times higher than in wild-type cerebellum, it should be noted that reverse transcribed cDNA of endogenous ataxin-3 was much longer than that of truncated ataxin-3[Q69]: it cannot be excluded the possibility that the longer cDNA template affected the initial speed for the amplification of the PCR product because of the secondary structure. (E) Western blot analysis of the endogenous CRAG expression in the cerebella of three different polyQ mice lines using a polyclonal anti-CRAG antibody. Cerebellar protein extracts from polyQ mouse lines and wild-type mice were loaded as indicated above each lane. The same blot was reacted with an anti-actin antibody, which detected the mouse β-actin protein, showing that loading was roughly equal in each lane. (F) The % ratio of the cerebellum to the whole brain weight that was measured at P20 and P80 using (b) line transgenic mice and their wild-type littermates.

Supplementary Figure 2. Torashima et al.

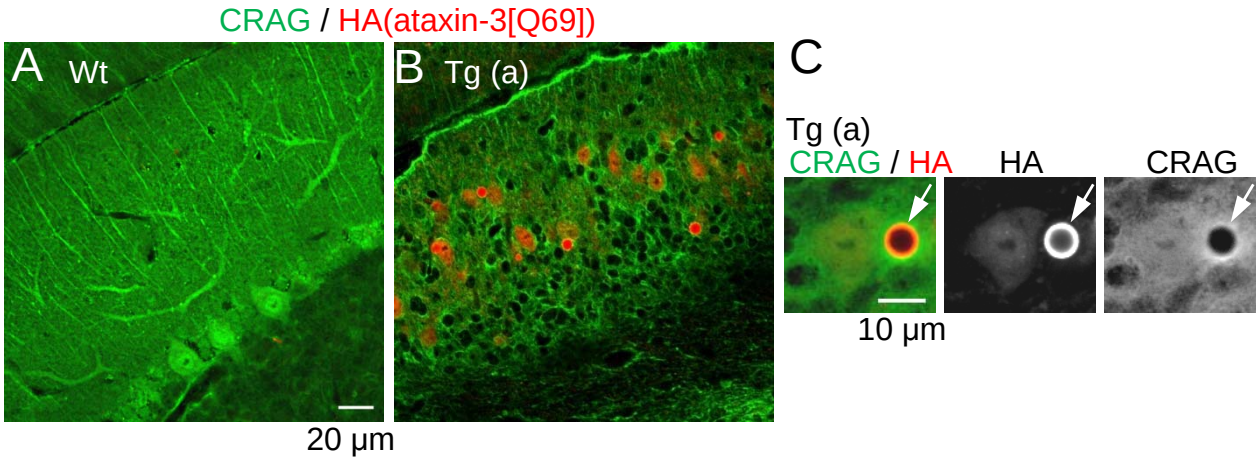

Supplementary Figure 2. Immunohistochemical analysis of endogenous CRAG and mutant ataxin-3.
(A-C) Cerebellar sections from wild-type (A) and transgenic (B, C) mice were double immunolabeled with anti-CRAG (green) and anti-HA (red) antibodies. A transgenic mouse of the (a) line at P80 and an age-matched littermate were used for the analysis. Enlarged images (C) show a polyQ inclusion surrounded by CRAG (arrows). Scale bars; 20μm (A) and 10 μm (C).

Supplementary Figure 3. Torashima et al.

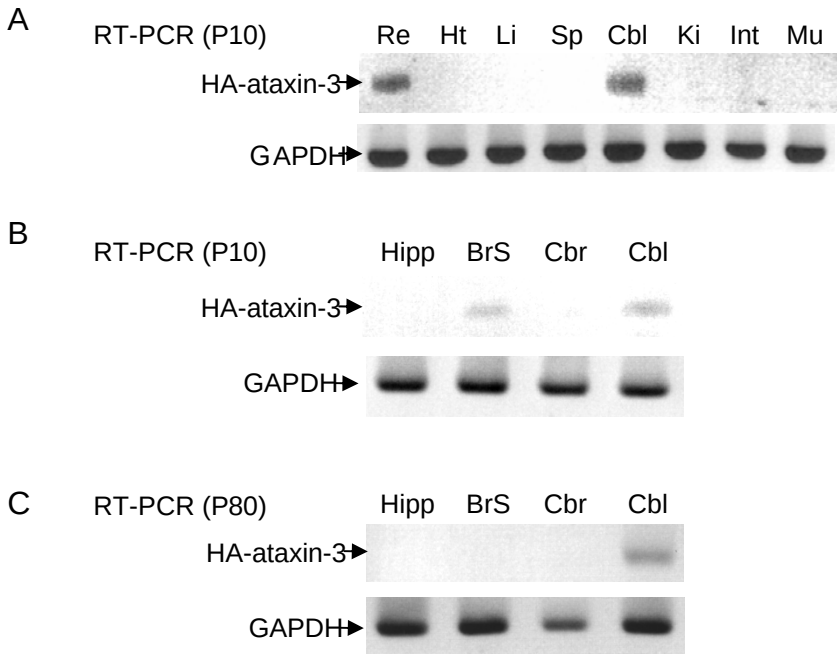

Supplementary Figure 3. Expression profile of ataxin-3[Q69] mRNA in various tissues.
Reverse transcriptase PCR (RT-PCR) was conducted to examine the transgene expression using various non-neuronal and neuronal tissues from (b) line polyQ mice at P10 and P80. Input levels were verified by amplifying glycelaldehyde-3-phosphate dehydrogenase GAPDH mRNA. (A) Presence of mutant ataxin-3 mRNA in the retina and cerebellum of a P10 polyQ mouse. (B, C) Presence of mutant ataxin-3 mRNA in the brain stem at P10 (B), but not P80 (C). The mRNA was detected exclusively in the cerebellum at P80. Re; retina, Ht; heart, Li; liver, Sp; spleen, Cbl; Cerebellum, Ki; Kidney, Int; Intestine, Mu; Muscle, Hipp; Hippocampus, BrS; Brain stem, Cbr; Cerebrum.

Supplementary Figure 4. Torashima et al.

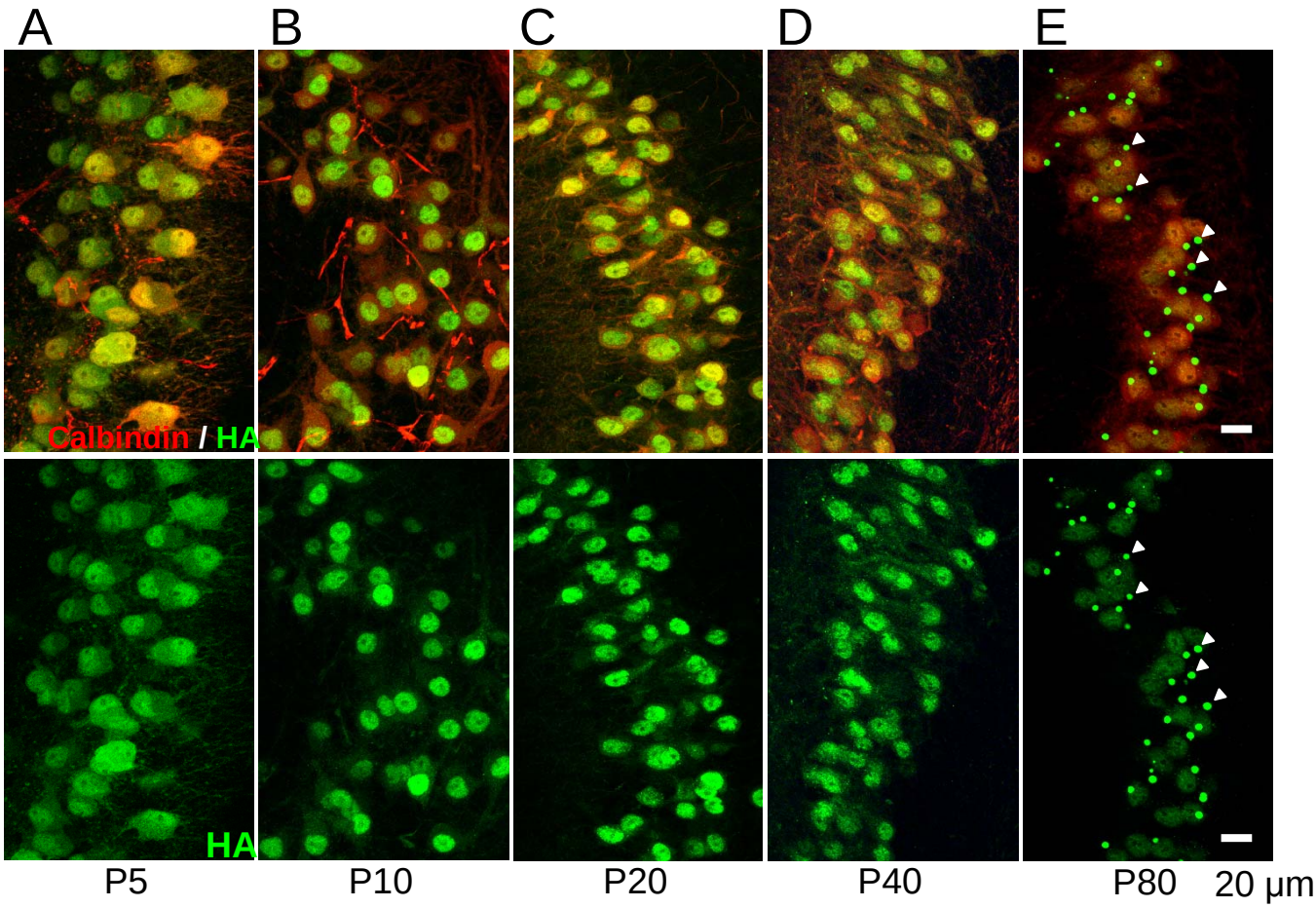

Supplementary Figure 4. Developmental change in the localization of polyQ aggregates in Purkinje cells.
Cerebellar sections were obtained from P5 (A), P10 (B), P20 (C), P40 (D) and P80 (E) polyQ mice [(b) line], and immunolabeled for HA tagged with ataxin-3[Q69] (green) and calbindin (red). Lower panels show only a green channel. Note that polyQ aggregates existed diffusely in both cytoplasm and nuclei at P5, while they were confined to the nuclei at P10 and thereafter. Small inclusion bodies were detected at P40, which drastically increased the size and number at P80 (arrowheads). Scale bar; 20μm.

Supplementary Figure 5. Torashima et al.

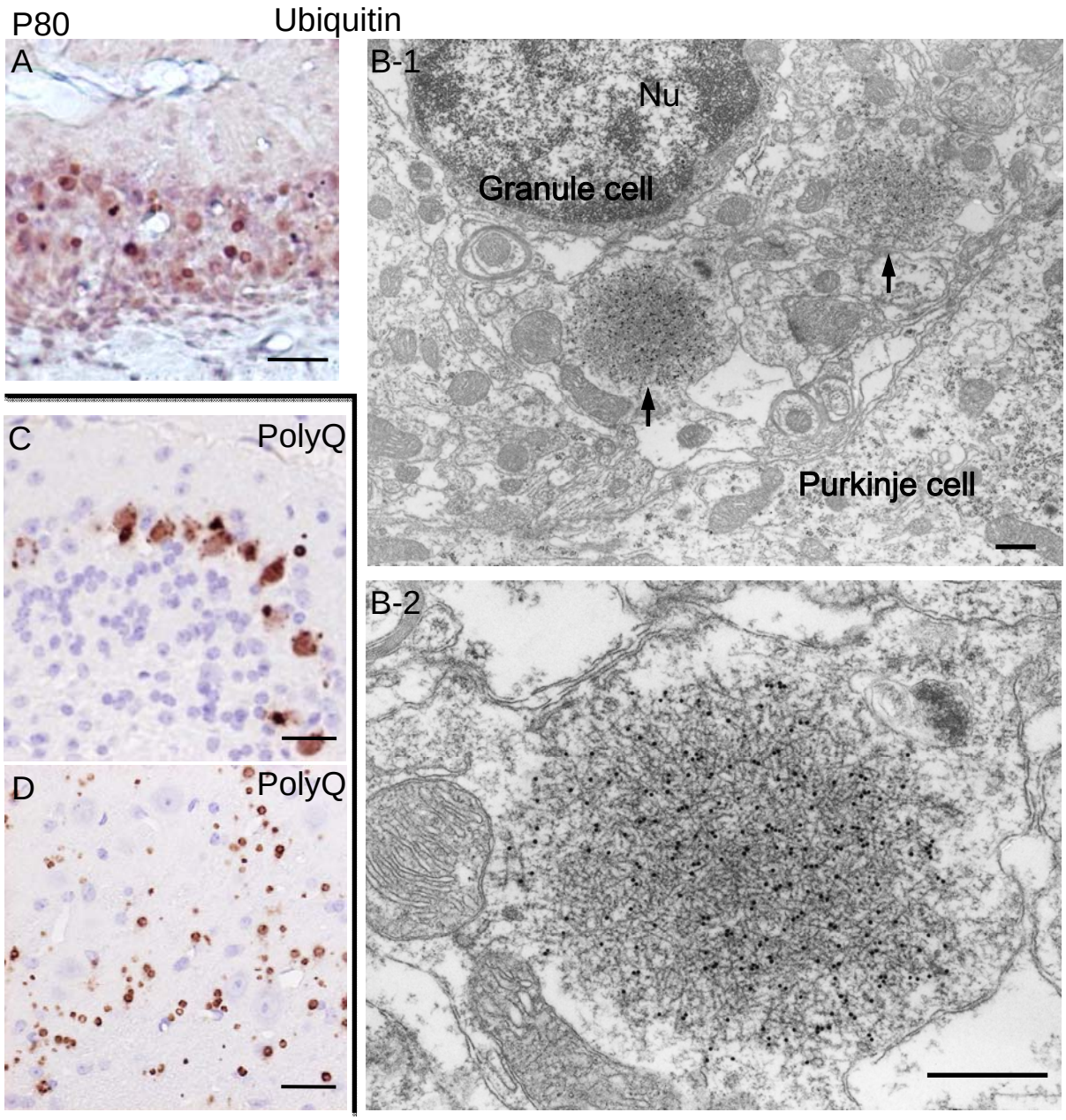

Supplementary Figure 5. Ubiquitination of polyQ inclusions.
(A-D) Immunolabeling of polyQ inclusions in P80 (b) line mutant Purkinje cells with anti-ubiquitin (A, B) and anti-expanded polyglutamine [clone; 1C2, (C, D)] antibodies. Inclusion bodies along the Purkinje cell layer were immunolabeled for ubiquitin (A) and expanded polyQ (C). Immunoelectron microscopic examination showed the presence of labeled inclusion bodies in an area between a granule cell and a Purkinje cell (B-1). They were frequently observed outside of or in the cytoplasm, but not in the nuclei of Purkinje cells. An enlarged image showed that the inclusion was filled with the abnormal filaments (B-2). Small inclusion bodies were present with 1C2 labeling at the axon terminals of Purkinje cells (D). Scale bars; 25 μm (A, C, D); 500 nm (B).

Supplementary Figure 6. Torashima et al.

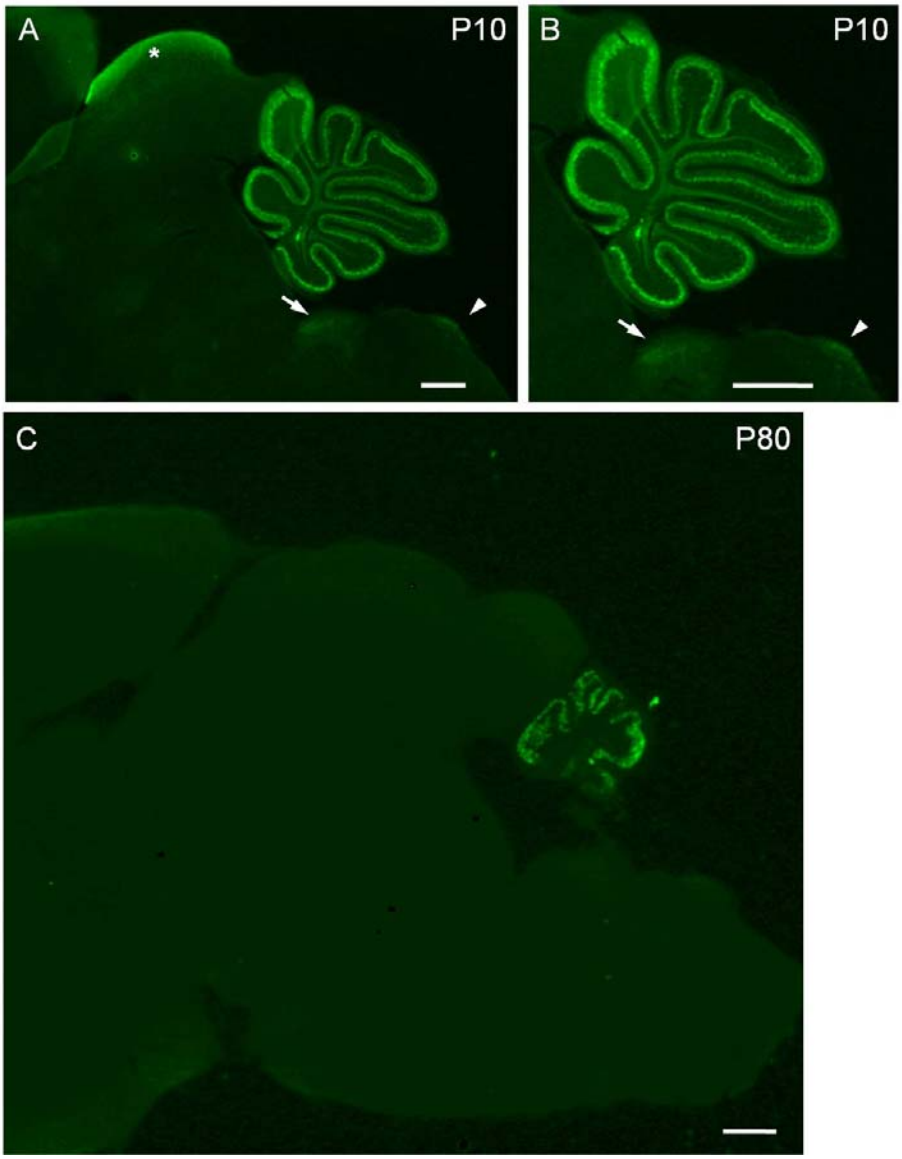

Supplementary Figure 6. Expression of mutant ataxin-3[Q69] in the hindbrain of polyQ mice. The (b) line polyQ mice at P10 (A, B) and P80 (C) were immunolabeled for HA tagged with mutant ataxin-3[Q69]. HA immunoreactivity was observed in the cerebellum at both P10 and P80. In addition to the cerebellum, P10, but not P80, polyQ mice expressed mutant ataxin-3 in the superior colliculus (A, asterisk), the medial vestibular nuclei (white arrows) and the cuneate nuclei (arrow heads). Scale bars; 500 μm.

Supplementary Figure 7. Torashima et al.

Supplementary Figure 7.
Representative footprints of polyQ mice treated with wild-type CRAG (CRAG$_{WT}$), NLS-sequence-mutated CRAG (CRAG$_{NLSmu}$) or GFP.

Supplementary Figure 8. Torashima et al.

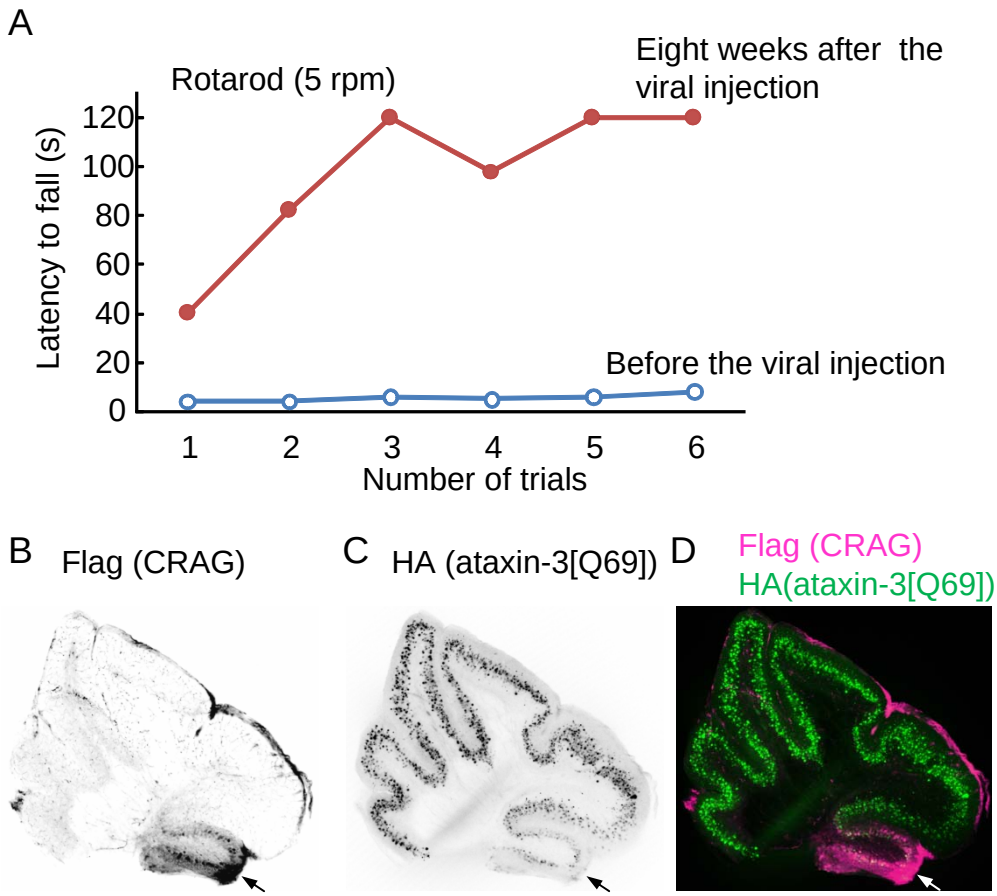

Supplementary Figure 8. An example of CRAG-mediated rescue of rotarod performance and removal of the inclusions in a (b) line polyQ mouse.
(A) Rotarod analysis of a polyQ mouse before and two months after CRAG treatment. The polyQ mouse showed poor rotarod performance before the lentiviral injection (open circles): the mouse fell down from the rod immediately after the start of the examination. Eight weeks after the injection of lentiviral vectors expressing CRAG, the rotarod performance substantially improved (closed circles). The rod speed was fixed at 5 rpm. Each animal was tested for a maximum of 120 s. (B-D) The cerebellar slice double immunolabeled for Flag tagged with CRAG (B) and HA tagged with ataxin-3[Q69] (C). A merged image is shown in (D). The vestiblocerebellum around lobule 10 (arrows) that expressed recombinant CRAG shows substantially lower immunoreactivity for HA (ataxin-3[Q69]) than other regions that did not express CRAG. Although recombinant CRAG was detected only in one lobule in this animal, overall, it was expressed in one to three lobules.

Supplementary Figure 9. Torashima et al.

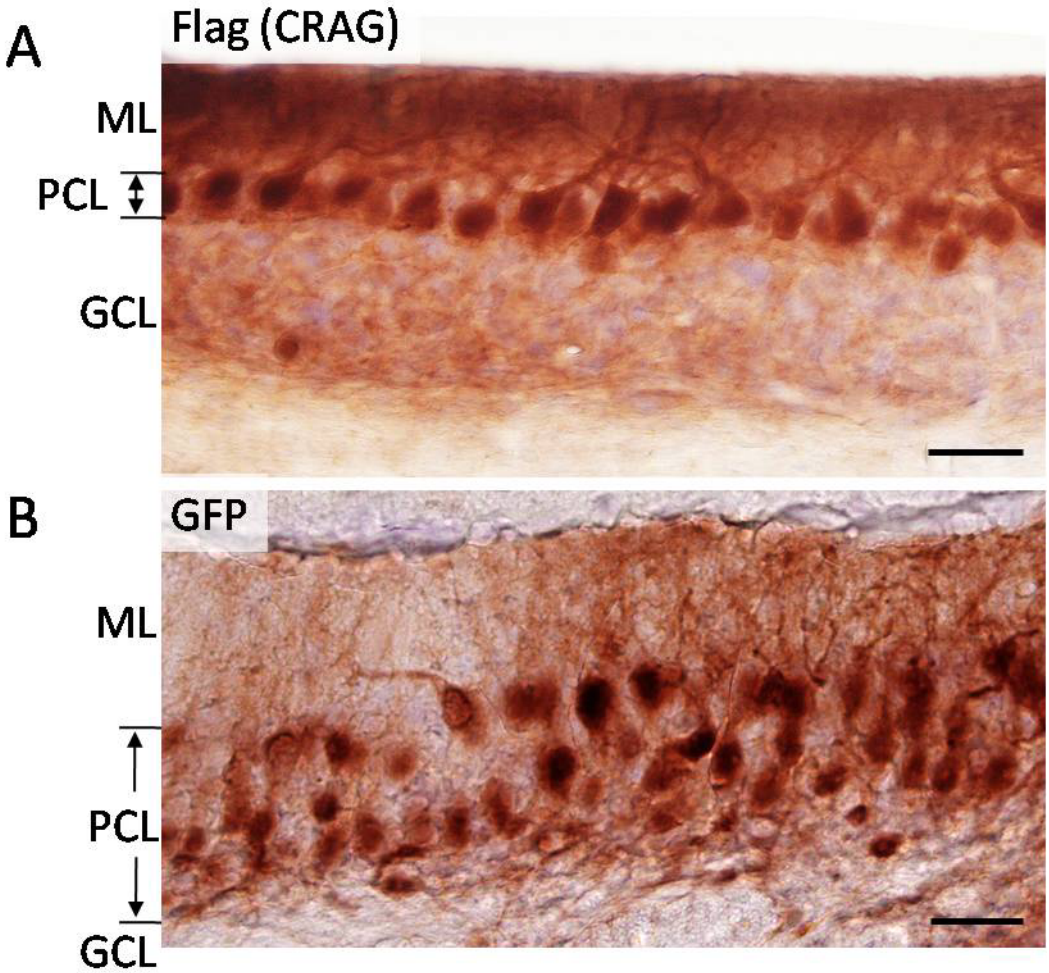

Supplementary Figure 9. Rescue of the arrangement of Purkinje cells upon CRAG expression in a polyQ mouse.
A polyQ mouse at P25 received an injection of lentiviral vectors expressing CRAG (A) or GFP (B). Eight weeks after the injection, the mouse was sacrificed, and the cerebellum was immunostained for Flag tagged with CRAG or GFP. Note that Purkinje cells expressing CRAG, but not GFP, line up beautifully to form a monolayer (arrows).

Supplementary Figure 10. Torashima et al.

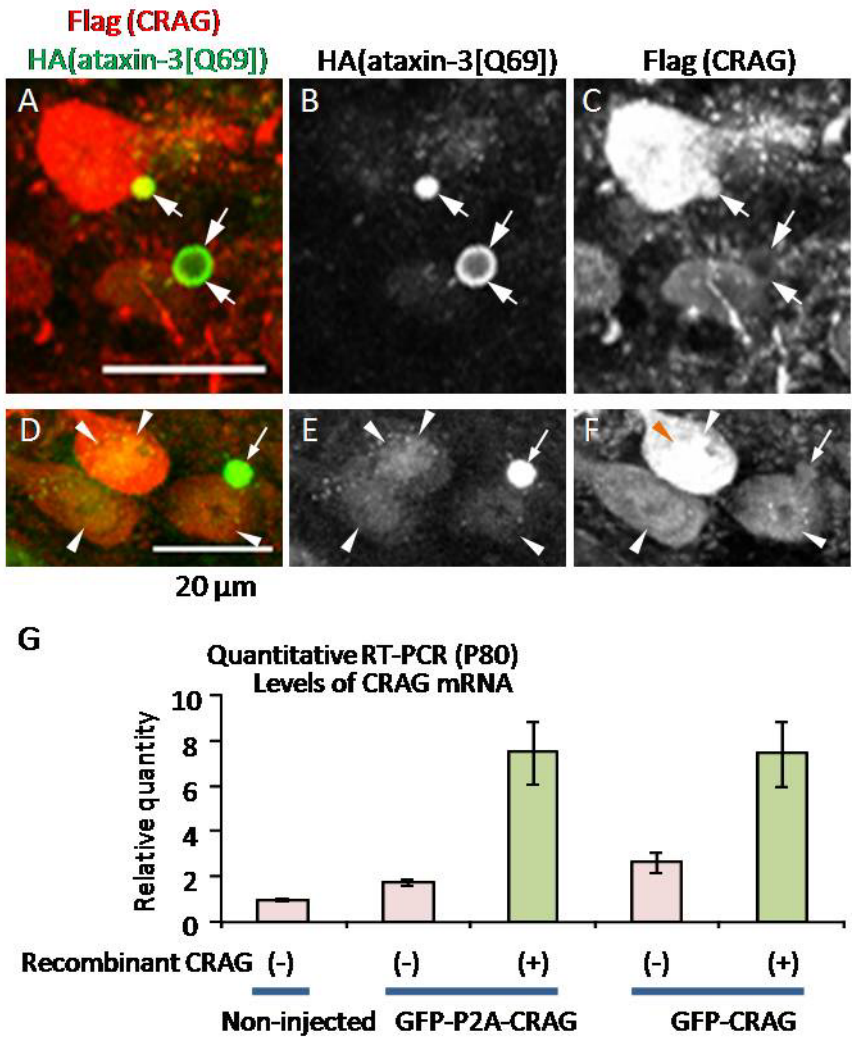

Supplementary Figure 10. Overexpression of recombinant CRAG in mutant Purkinje cells. (A-F) Colocalization of CRAG with polyQ inclusions. CRAG and polyQ were visualized by double immunolabeling for Flag and HA, respectively. Immunoreactivity for CRAG was detected on the inclusions (arrows) and aggregates (arrowheads) immunolabled for HA. (G) A quantitative RT-PCR result showing the levels of CRAG in non-transduced and transduced lobules of the polyQ mouse cerebellum. To detect CRAG-expressing lobules without immunostaining, GFP was fused with CRAG directly (GFP-CRAG) or indirectly (GFP-P2A-CRAG) via the Picornavirus 'self-cleaving' 2A peptide sequence (P2A) (Szymczak *et al*, 2004). Using lentiviral vectors, one of the GFP-CRAG fusion proteins was expressed in polyQ mouse cerebellum. Eight weeks after the injection, cerebellar slices were taken and CRAG-expressing lobules in the cerebellum were identified by GFP fluorescence. Total mRNA was isolated from lobules with and without CRAG expression, followed by quantitative RT-PCR analysis after reverse transcription of CRAG mRNA. The data from eight runs of real-time PCR using 2 animals were normalized with the values of non-injected polyQ mouse cerebellum. Note that the expression levels of CRAG mRNA in transduced lobules were ~7 times higher than in non-injected lobules. Because transduced and non-transduced lobules were separated visually, some cells close to the boarder in non-transduced lobules probably express recombinant CRAG. This could explain the slight increase in the levels of CRAG mRNA in non-transduced lobules.

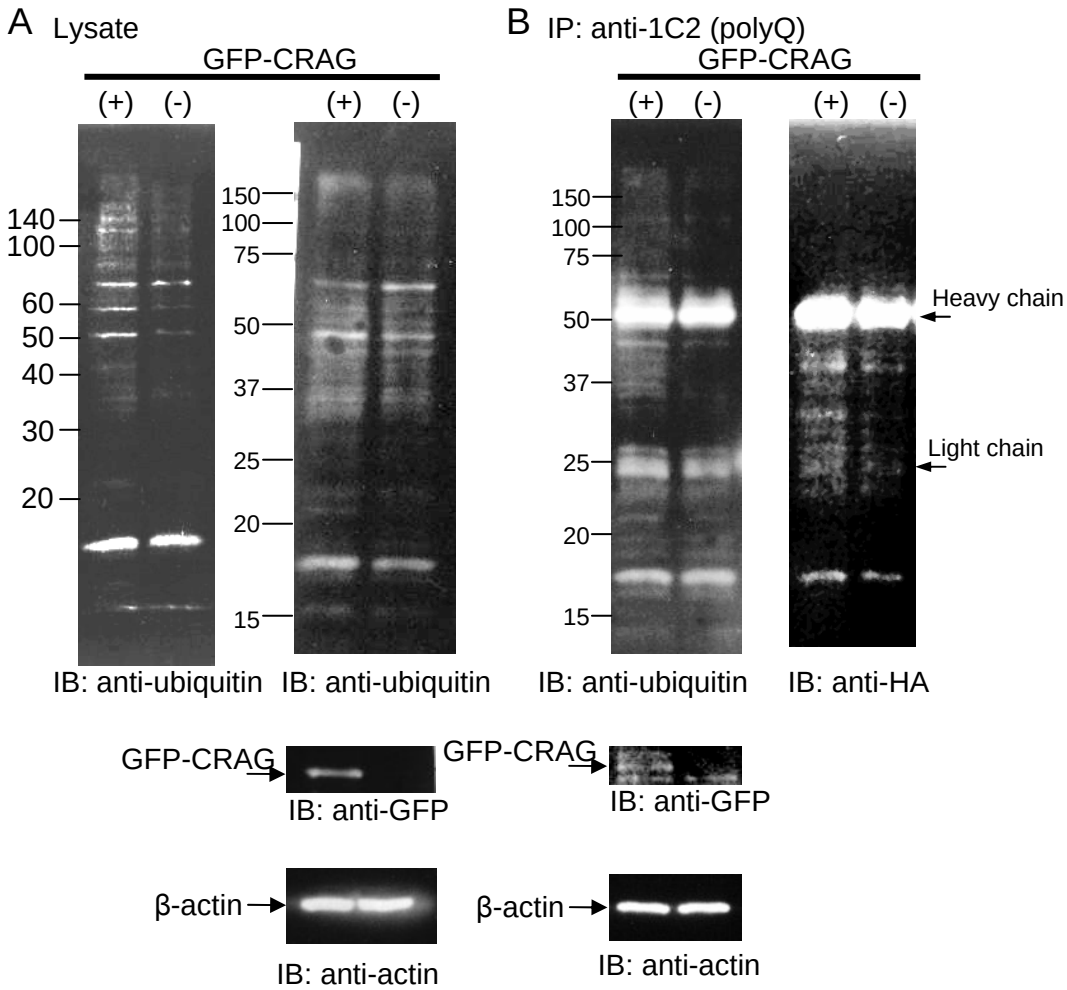

Supplementary Figure 11. Enhancement of polyQ ubiquitination in the lobules expressing GFP –CRAG.

Lentiviral vectors expressing GFP-CRAG were injected to the cerebellar cortex of polyQ mice. Fourteen days after the injection, the mice were used for the analysis. (A) Enhanced ubiquitination in the lobules expressing GFP-CRAG. Protein extracts from lobules with or without recombinant GFP-CRAG were loaded as indicated above each lane. The results obtained from two mice were presented. The right blot was also reacted with anti-GFP and anti-actin antibodies. The ubiquitination was apparently enhanced by CRAG delivery. (B) Increase in the ubiquitination of polyQ. Using anti-expanded polyQ (1C2) antibody, polyQ (ataxin-3[Q69]) was immunoprecipitated from transgenic mouse lobules with or without GFP-CRAG and analyzed by immunoblot for ubiquitin (left) and HA (right). The same blot was reacted with anti-GFP and anti-actin antibodies. Note that GFP-CRAG was coimmunoprecipitated with polyQ. The experiments were repeated three times using three animals and the representative results were presented.

Supplementary Video 1. Ataxic gate of the PolyQ mice (P80).
A polyQ mouse expressing mutant ataxin-3[Q69] in Purkinje cells shows severe ataxia.

Supplementary Video 2. Rescue of the ataxic phenotype upon lentivector-mediated expression of CRAG.
A)Typical gating pattern of untreated polyQ mice at P80.
B)Typical gating pattern of polyQ mice eight weeks after treatment with lentivectors expressing CRAG.
C)Typical rotarod performance of untreated polyQ mice at P80.
D)Typical rotarod performance of polyQ mice eight weeks after treatment with lentivectors expressing CRAG.

Supplementary Methods

Generation of transgenic mice

The transgene that was used to generate polyQ mice encodes NH_2-terminal–truncated ataxin-3 with Q69 together with an NH_2-terminal HA epitope (Yoshizawa *et al*, 2000). Ataxin-3 lacks the 286 NH_2-terminal amino acid residues. This mutant ataxin-3 cDNA was inserted into the BamHI site of pL7ΔAUG (Oberdick *et al*, 1990). The original ATG start codon situated in exon 2 was mutated to inhibit the expression of exons 1-3 of the L7 gene. The resulting plasmid was digested with *Hind*III and *Eco*RI, and the linearized L7-mutant ataxin-3 construct separated from the vector by electrophoresis. The purified L7- mutant ataxin-3 transgene was injected into fertilized eggs. We used only the wild-type and heterozygous polyQ mice for the experiments. Transgenic mice that express truncated ataxin-3 with unexpanded CAG repeats were not generated because such a construct had no toxicity in BHK-21 cells (Yoshizawa *et al*, 2000), and the transgenic mice showed no abnormal phenotype (Ikeda *et al*, 1996). Basically we used male mice for the experiments. However, as differences of phenotypes between genders in each polyQ mice line are essentially indistinguishable, some results involve data obtained using female mice.

Rotarod test

The motor control ability of the mice was assessed by a rotarod test with two different paradigms. The Rota-Rod Treadmill (Muromachi kikai, Tokyo, Japan) consists of a gridded plastic rod (3 cm in diameter, 10 cm long) flanked by two large round plates (50 cm in diameter). The rod accelerated in 3 min from 0 rpm to 40 rpm or rotated stably with a speed of 5 rpm. Mice were assessed with the accelerating paradigm just before and every two weeks up to eight weeks or with the fixed paradigm eight weeks after the viral injection. In each test, the mice were subjected to the four trials with a 30 min of rest between trials, and the average time to fall off the rod was determined. The data (average ± SEM) collected for each group of animals were plotted on the graph.

Histological methods

Mice were perfused transcardially with a fixative containing 4 % formaldehyde (plus 0.1 % glutaraldehyde for the electron microscopic study) in 0.1 M phosphate buffer after being deeply anesthetized by diethyl ether inhalation(Torashima *et al*, 2006b). The cerebellum was removed and postfixed in the same fixative for three hours. For immunostaining, the cerebellum was cut into 40- to 100-μm sagittal sections using a microslicer (DOSAKA DTK-1000, Kyoto, Japan). Floating sections were immunostained with rabbit polyclonal anti-calbindin D-28K (1:200; Sigma, St Louis, MO) and mouse monoclonal anti-HA (1:1,000; InvivoGen, CA) or rabbit polyclonal anti-ubiquitin (1:1,000; DAKO, Carpinteria, CA), and visualized with Alexa fluor 568- and Alexa-488-conjugated (10 μg/ml; Invitrogen) or peroxidase-tagged secondary antibodies. Control sections were stained with normal mouse IgG (1 μg/ml) or by omitting primary antibodies.

We also prepared paraffin-embedded tissue sections, and subjected them to Klüver-Barrera (KB; cresyl violet and luxol fast blue) staining and staining for expanded polyglutamine (1C2; mouse monoclonal, Chemicon, Temecula, CA; 1:10,000) with formic acid pretreatment(Hayashi *et al*, 2003). For the post-embedding immuno-electron microscopic study, 1 mm^3 tissue blocks were fixed with 4% formaldehyde and 1% glutaraldehyde solution for one day, osmified and embedded in epoxy resin. Ultrathin sections placed on Ni glids were immunolabeled with anti-ubiquitin (1:200) or control rabbit antiserum, and 15-nm gold-tagged anti-rabbit IgG (Fc) (1:20, Amersham; RPN 425, USA), and observed under an electron microscope (JEM 1010, JEOL)(Yamaguchi *et al*, 2000).

RT-PCR analysis

Quantitative RT-PCR was performed on a Thermal Cycler Dice TP800 system (Takara Bio) using

SYBR Premix Ex Taq II (Takara) with cycles of 95ºC for 5 s and 60ºC for 30s. GAPDH was used as an internal standard. The cycle threshold value, which was determined using the second derivative, was used to calculate the normalized expression of the indicated genes using GAPDH as a reference gene. The following primer pairs were used: GAPDH, 5'-tgtgtccgtcgtggatctga-3' and 5'-ttgctgttgaagtcgcaggag-3'; endogenous ataxin-3', 5'-ggacctatcaggacagagttc-3', 5'-catggagctcgtatgtcagata-3'; Calbindin, 5'-ctctgatcacagcctcacagtt-3', 5'-gcagaagctcctggatcaagtt-3'; CRAG, 5'-gcgcaacctatgggctcaa-3', 5'-tgatgtgcacagctgggatg-3'.

Western blot analysis

Brain tissue was solubilized in a lysis buffer containing 50 mM PBS, 5 mM EDTA, 0.4% Triton X-100 supplemented with a cocktail of protease inhibitors (Nacalai tesque). Samples were sonicated and determined the protein concentrations using a NIPA kit (Non-interfering Protein Assay, Calbiochem). Samples were incubated for 5 min at 95˚C and loaded to SDS-PAGE gels. Then, proteins were transferred onto PVDF membrane (Millipore), followed by blocking with 4% nonfat skim milk in Tris-buffered saline containing 0.2% Tween-20. Blots were incubated with polyclonal anti-CRAG or monoclonal anti-actin antibodies at 1 : 5000 dilution. The secondary antibodies were HRP-conjugated anti-rabbit or anti-mouse IgG (Bio-Rad), respectively, at 1 : 4000 dilution. Immunoreactive bands were visualized using enhanced chemiluminescence reagent (ECL plus, Amersham). We could not assess the expression levels of ataxin-3[Q69] protein by Western blot because many tissues, including the brain, of wild-type mice (and mutant mice as well) possess a protein of a size (~18 kD), comparable to HA-ataxin-3[Q69], that cross-reacted with anti-HA antibodies purchased from three suppliers [Sigma (anti-rabbit), Roche (anti-rat) and Invivogen (anti-mouse)]. Moreover, the truncated ataxin-3 that was used for generation of the polyQ mice lacks the epitope for a commercial monoclonal antibody (clone 1H9).

Virus preparation and cerebellar injection

Vesicular Stomatitis Virus-G protein (VSV-G) pseudotyped lentiviral vectors provided by St. Jude Children's Research Hospital (Hanawa *et al*, 2002) were used in this study. The vectors were designed to express 3xFlag-tagged CRAG, 3xFlag-tagged $CRAG_{NLSmu}$, GFP-3xFlag-tagged CRAG, GFP-P2A-3xFlag-tagged CRAG or GFP under the control of the cytomegalovirus (CMV) promoter or murine stem cell virus (MSCV) promoter. In cerebellar neuronal cultures, a Purkinje cell – specific L7 promoter was used. The virus vectors were produced as described previously (Torashima *et al*, 2007; Torashima *et al*, 2006a). The PolyQ mice and their littermates were injected with the viral vectors at four weeks of age. Each mouse was injected intraperitoneally with sodium pentobarbital (40 mg/kg body weight) to produce deep anesthesia. Four microliters of virus solution was injected at the surface of the cerebellar vermis using a micropump as previously reported(Torashima *et al*, 2006a). Most of the solution did not soak into the cortex and spread through the subarachnoidal space over the cerebellum.

Acquisition and analysis of fluorescent inclusions

Fluorescent images of inclusions in cerebellar slices and cultures were obtained by a confocal laser-scanning microscope (LSM 5 PASCAL; Zeiss, Oberkochen, Germany) or a cooled CCD camera attached to a fluorescence microscope (DMI6000 B; Leica, Nussloch, Germany), respectively. The same exposure time was used to acquire fluorescent images from non-treated control, GFP-expressing and CRAG-expressing Purkinje cells. In the confocal microscopic analysis, cerebellar slices were scanned at 1 μm intervals, and 10 sections were projected. Inclusions were detected by threshold-based segmentation. The same threshold value, obtained from a control sample, was used

for inclusion detection in GFP- or CRAG-treated samples as previously described (Hirai *et al*, 2003). The number, size and intensity of inclusions were determined using IPLab imaging software (Scanalytics).

Cerebellar neuronal culture

Dissociated cerebellar neuronal cultures were prepared from P0 mouse pups according to a published protocol (Furuya et al, 1998). In brief, 5.0×10^6 cells/ml (200,000 cells per well in 40 μl) were plated onto plastic coverslips (13.5 mm in diameter; Sumilon MS-92132; Sumitomo Bakelite, Tokyo, Japan) coated with poly-L-ornithine and placed in a humidified CO_2 incubator (5% CO_2 at 37°C). This culture contained ~70% of neuron-specific enolase (NSE)-positive cells. All other cells were glial fibrillary acidic protein-positive. The ratio of granule cells to Purkinje cells was ~20:1. Eight hundred microliters of serum-free culture medium was added to each well after 2 hr. The medium was composed of a DMEM-nutrient mixture of Ham's F-12 supplemented with bovine insulin (10 μg/ml), bovine serum albumin (100 μg/ml), gentamicin (5 μg/ml), glutamine (200 μg/ml), human apotransferrin (100 μg/ml), progesterone (40 nM), putrescine (100 nM), sodium selenite (30 nM), and triiodothyronine (0.5 ng/ml).

Supplementary references

Hanawa H, Kelly PF, Nathwani AC, Persons DA, Vandergriff JA, Hargrove P, Vanin EF and Nienhuis AW (2002) Comparison of various envelope proteins for their ability to pseudotype lentiviral vectors and transduce primitive hematopoietic cells from human blood. *Mol Ther* **5:** 242-251

Hayashi M, Kobayashi K and Furuta H (2003) Immunohistochemical study of neuronal intranuclear and cytoplasmic inclusions in Machado-Joseph disease. *Psychiatry Clin Neurosci* **57:** 205-213

Hirai H, Launey T, Mikawa S, Torashima T, Yanagihara D, Kasaura T, Miyamoto A and Yuzaki M (2003) New role of delta2-glutamate receptors in AMPA receptor trafficking and cerebellar function. *Nat Neurosci* **6:** 869-876

Oberdick J, Smeyne RJ, Mann JR, Zackson S and Morgan JI (1990) A promoter that drives transgene expression in cerebellar Purkinje and retinal bipolar neurons. *Science* **248:** 223-226

Szymczak AL, Workman CJ, Wang Y, Vignali KM, Dilioglou S, Vanin EF and Vignali DA (2004) Correction of multi-gene deficiency in vivo using a single 'self-cleaving' 2A peptide-based retroviral vector. *Nat Biotechnol* **22:** 589-594

Torashima T, Koyama C, Higashida H and Hirai H (2007) Production of neuron-preferential lentiviral vectors. *Nat Protocol***:** DOI: 10.1038/nprot.2007.1089

Torashima T, Okoyama S, Nishizaki T and Hirai H (2006a) In vivo transduction of murine cerebellar Purkinje cells by HIV-derived lentiviral vectors. *Brain Res* **1082:** 11-22

Torashima T, Yamada N, Itoh M, Yamamoto A and Hirai H (2006b) Exposure of lentiviral vectors to subneutral pH shifts the tropism from Purkinje cell to Bergmann glia. *Eur J Neurosci* **24:** 371-380

Yamaguchi H, Maat-Schieman ML, van Duinen SG, Prins FA, Neeskens P, Natte R and Roos RA (2000) Amyloid beta protein (Abeta) starts to deposit as plasma membrane-bound form in diffuse plaques of brains from hereditary cerebral hemorrhage with amyloidosis-Dutch type, Alzheimer disease and nondemented aged subjects. *J Neuropathol Exp Neurol* **59:** 723-732

Yoshizawa T, Yamagishi Y, Koseki N, Goto J, Yoshida H, Shibasaki F, Shoji S and Kanazawa I (2000) Cell cycle arrest enhances the in vitro cellular toxicity of the truncated Machado-Joseph disease gene product with an expanded polyglutamine stretch. *Hum Mol Genet* **9:** 69-78